# Post-Assembly Modification of Phosphine Cages Controls Host-Guest Behavior

Charlie T. McTernan, Tanya K. Ronson, Jonathan R. Nitschke*

Department of Chemistry, University of Cambridge, Lensfield Road, Cambridge, CB2 1EW, United Kingdom

*Supporting Information Placeholder*

**ABSTRACT:** We report the design, synthesis and post-assembly modification of a new phosphine-paneled supramolecular cage framework, whose anion binding ability can be modified rationally through selective post-assembly functionalization. The parent phosphine-paneled cage can be modified *in situ* through oxidation, methylation, or auration. These covalent and coordinative modifications to the exterior of the cage strongly influence the guest binding properties of the host.

The post-translational modification of proteins[1] or methylation of DNA[2,3] can dramatically alter the properties of the original biomolecules.[4] Biological systems can thus adapt their function in response to environmental triggers.[5] These modifications can cause either localized changes or large-scale structural alterations, and are involved in processes as diverse as sight, signaling and selective transport in cells.[6-8] The ubiquity of post-synthetic modification in biological processes has inspired a range of adaptive synthetic molecular systems, including novel switches, machines, and materials that respond to stimuli on the molecular level.[9-11] Post-assembly modification (PAM) can tune the properties of metal-organic frameworks[12], polymers[13] and crystals[14] allowing a single parent architecture to perform a variety of functions. A wide range of stimuli,[15] including pH change,[16] guest binding,[17] and ligand photoisomerization[18] have been used to destroy or transform supramolecular architectures,[19] but the use of covalent bond formation is less common, as many supramolecular architectures are observed to decompose under the conditions required to form covalent linkages.[20]

Interest has grown in designing supramolecular systems which tolerate PAM reactions,[21] with a range of cycloaddition, metathesis, acylation and alkylation reactions having been explored.[22] Light has been used to trigger guest release,[23] and the alkylation of covalent organic frameworks has been shown to modify their gas absorption ability,[24] but the use of PAM to modify the guest binding abilities of metal-organic cages has not yet been exploited.[25]

Metal-organic cages are commonly formed from hydrocarbon-based panels,[26] with heteroatom incorporation often restricted to metal binding motifs.[27] The incorporation of heteroatom-containing motifs such as azaphosphazines,[28] porphyrins,[29] or hydrogen bonding motifs[30] has led to functions that include the stabilization of internal coordination complexes and catalysis.[31]

Here we present a new metal-organic cage framework, based upon a tritopic phosphine-containing ligand, and incorporating nickel(II), iron(II) or zinc(II). The phosphine groups within the walls of these cages allow PAM by alkylation, oxidation, or auration. These cage modifications alter the anion-binding properties in solution, providing a way to tune the binding ability of molecular capsules *in situ*.

The addition of zinc bis(trifluoromethanesulfonyl)imide (triflimide, $Tf_2N^-$) to tritopic ligand **1** resulted in the formation of capsule **2**, a $Zn_4L_4$ tetrahedron (Figure 1). This capsule makes use of the robust triazole-pyridine bidentate coordination motif developed by Lusby.[32] We chose the triazole-pyridine motif as we expected it to exhibit greater stability to the PAM reactions we wished to explore (i.e. oxidation) than the iminopyridine motif.[16c,19,21,26b,28] Interestingly, we observed that $Et_3NHCl$ (initially remaining from the reduction of the phosphine oxide precursor to **1**, Supporting Information Sections S6 and S10) was required for the clean formation of tetrahedron **2**. Addition of tetrabutylammonium chloride alone was not sufficient to cause clean assembly, suggesting that the slightly greater acidity of $Et_3NHCl$ was a necessary condition (Figure S119). ESI-MS confirmed the $Zn_4L_4$ composition of **2**, and NMR spectroscopy was consistent with the formation of a cage with *T* symmetry.

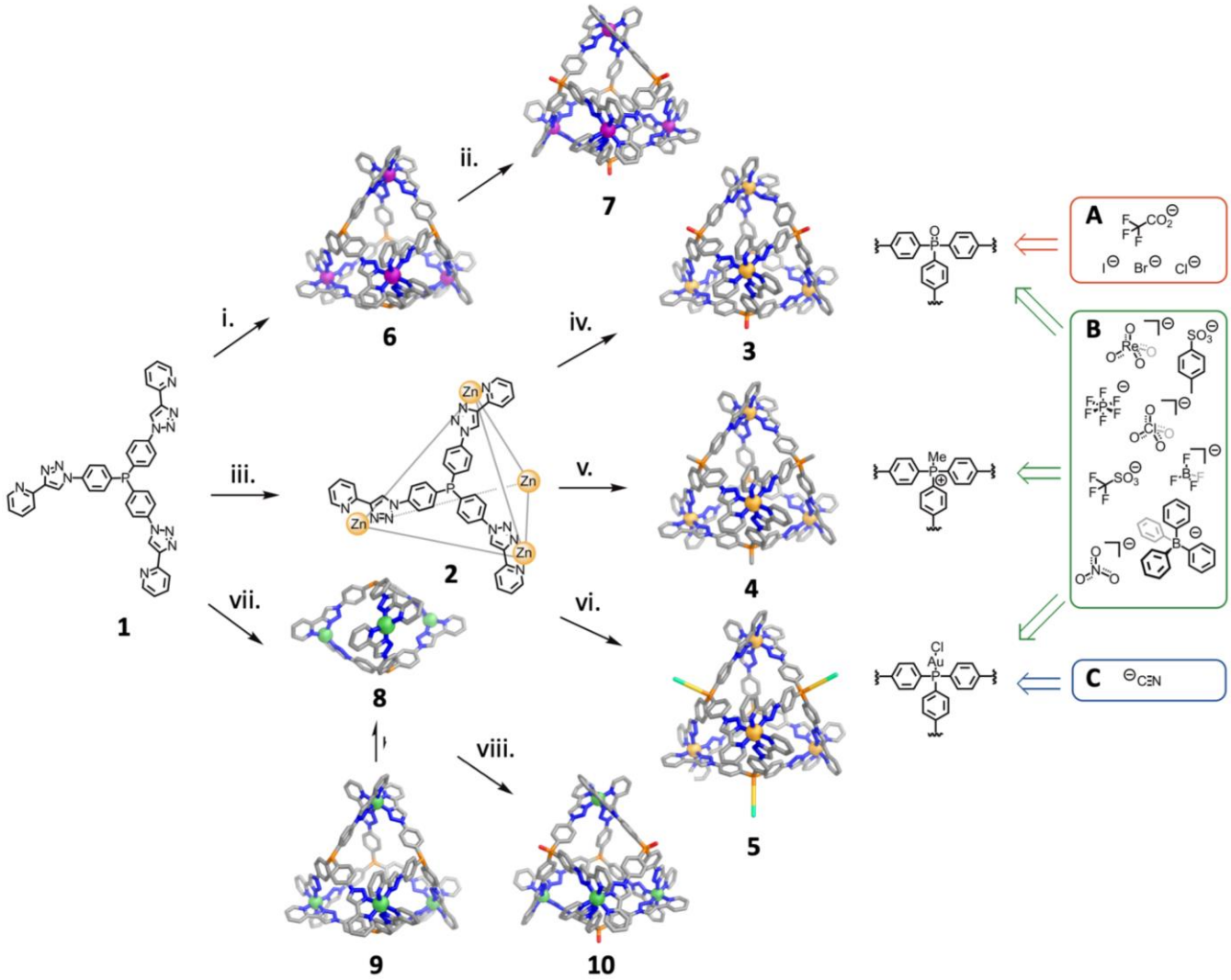


**Figure 1.** Synthesis of phosphine-paneled cages. **i**. Iron(II) triflimide (1.0 equiv), MeCN, 70 °C, 1 hour. **ii**. $H_2O_2$ (6 equiv), MeCN, r.t., 1 hour. **iii**. Zinc triflimide (1.2 equiv), MeCN, 70 °C, 1 hour. **iv**. $H_2O_2$ (16 equiv), MeCN, r.t., 16 hour. **v**. MeI (225 equiv), $LiNTf_2$ (25 equiv), MeCN, 70 °C, 1 hour. **vi**. (DMS)AuCl (8 equiv), MeCN, 70 °C, 1 hour. **vii**. Nickel(II) triflimide (1.0 equiv), MeCN, 70 °C, 1 hour. **viii**. $H_2O_2$ (6 equiv), MeCN, r.t., 16 hour. Anions in box **B** bound to all cages. Anions in the box **A** bound exclusively to phosphine oxide cage **3**; cyanide in **C**, only to aurated cage **5**.

$Et_3NHCl$ was not required for the clean formation of $Zn_4L_4$ cages **3** and **4** (i.e. Figure 2b) from the corresponding ligands (Figures S49 and S60). Additionally, when PAM experiments (as described below) were performed, cages **3**, **4** and **5** were observed to form cleanly from **2** in the absence of $Et_3NHCl$.

When iron(II) triflimide was used in place of zinc triflimide, the analogous $Fe^{II}_4L_4$ cage **6** was formed. However, in the case of nickel(II) triflimide, mass spectrometry (Figure S76) showed the dominant species to be a $Ni^{II}_3L_2$ sandwich complex **8** instead of the expected $Ni^{II}_4L_4$ tetrahedral capsule **9**, although both species could be detected by HRMS (Figures S78 and S79). Although the tetrahedral co-ordination postulated for nickel(II) in **8** is unusual, it is not unheard of.[33,34] Interestingly, this equilibrium was not observed in the case of $Ni^{II}_4L_4$ tetrahedron **10**, assembled from the corresponding phosphine oxide ligand and nickel(II) triflimide (Figures S83-S87), with no corresponding $Ni^{II}_3L_2$ species seen by HRMS. This suggests that subtle structural variations can significantly perturb the relative stabilities of $Ni^{II}_3L_2$ sandwich **8** and $Ni^{II}_4L_4$ tetrahedron **9**.

Having established the generality of $M^{II}_4L_4$ cage preparation across iron, zinc, and nickel, we focused our investigations on PAM reactions of zinc phosphine cage **2**. Three transformations representative of phosphine chemistry were targeted: oxidation from phosphine to phosphine oxide, phosphine metalation to form transition metal complexes, and the formation of phosphonium salts through alkylation.

Phosphine oxide cage **3** was prepared directly from the corresponding phosphine oxide ligand (Supporting information Section S6) and zinc triflimide, as a reference to gauge the success of the formation of **3** from **2**. ESI-MS confirmed the composition of **3**, and NMR spectroscopy was consistent with a $Zn_4L_4$ structure with *T* symmetry. We then probed the direct addition of hydrogen peroxide as a means to transform

cage **2** to cage **3**.[35] The addition of $H_2O_2$ (16 equiv) to **2** led, within 10 minutes, to the formation of several intermediate species (Figure 2b). After 16 hours at 25 °C these species disappeared, forming cage **3**, whose NMR spectra matched those of a sample prepared directly from the phosphine oxide ligand, indicating that *in situ* oxidation occurred cleanly (Figure 2). $Fe^{II}_4L_4$ phosphine cage **6** was also cleanly oxidized *in situ* when treated with $H_2O_2$ (Figures S5-S7), forming phosphine oxide cage **7**. Treatment of the mixture of $Ni^{II}_3L_2$ sandwich **8** and $Ni^{II}_4L_4$ tetrahedron **9** with $H_2O_2$ also resulted in the formation of phosphine oxide $Ni^{II}_4L_4$ cage **10**, although the process did not proceed as cleanly (Figures S8-S11).

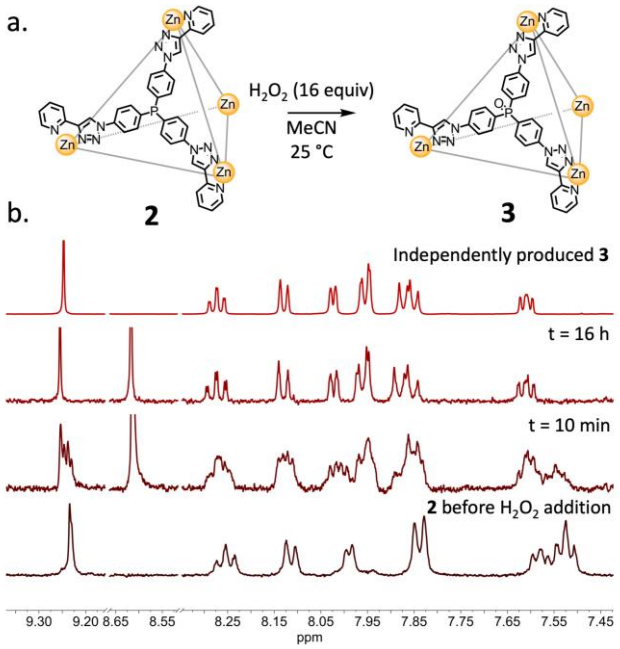


**Figure 2.** (a) Oxidation of phosphine cage **2** to phosphine oxide cage **3**; (b) $^1$H NMR spectra tracking this transformation over time. The peak at 8.6 ppm is due to $H_2O_2$.

We next investigated whether the triaryl phosphine groups on the walls of cage **2** could be used as a ligand for various metals.[36] Although no binding was observed for different sources of copper, palladium, rhodium and ruthenium (Table S1), cage **2** was observed to react with chloro(dimethyl sulfide)gold(I) ((DMS)AuCl) in solution to form cage **5** (Figure 1vi). The binding of four AuCl units per cage was confirmed by ESI-MS (Figures S67, S68). After binding of AuCl the cage no longer reacted with $H_2O_2$. No decomposition or conversion to the phosphine oxide was observed after 16 hours at room temperature, in contrast to the behavior of free phosphine cage **2**. In this instance, AuCl acts a protecting group for the phosphine (Figure S3).

The formation of cage **4**, based on four phosphonium salt panels, was then investigated. Phosphine ligand **1** underwent methylation to form a phosphonium salt (Figure S4), which then reacted with zinc triflimide to form the corresponding $Zn_4L_4$ cage. NMR and ESI-MS data (Figures S60-65, S56-59) were consistent with the proposed structure.

Initial attempts at *in situ* methylation of cage **2** led to cage decomposition. We hypothesized that the iodide released upon reaction with methyl iodide interfered with the assembly of cage **5**; indeed phosphonium cage **4** was observed to decompose upon addition of tetrabutylammonium (TBA) iodide (Figure S12). To counter this problem the *in situ* methylation reaction was performed in the presence of excess lithium triflimide (25 equiv), which was found to prevent the disassembly of phosphonium salt cage **4** during the course of the reaction, and so allow successful *in situ* methylation (Figure 1iv-vi).

Phosphine oxide $Fe^{II}_4L_4$ cage **11** was prepared from $FeSO_4$ in water (Figure S102), suggesting that rules for the design of aqueous metal-organic cages are applicable beyond the pyridyl-imine structures originally studied.[37] X-ray quality crystals of **11** were grown by slow diffusion of acetonitrile into an aqueous solution (Figure 3a).

X-ray quality crystals of phosphonium cage **4** (Figure 3b) and its nickel analogue **12** (formed from nickel triflimide in MeCN, Figure 3c) were also grown, in these cases by slow diffusion of benzene into a solution of the corresponding cage in MeCN. These structures confirmed the tetrahedral $M^{II}_4L_4$ architectures of the cages, and showed that the differently charged and functionalized ligands had limited structural effect on the tetrahedral framework (Figure 3). The phosphine panels were always found to be convex, and metal-metal distances comparable.

Having investigated the generality of cage formation based upon a single, adaptable, parent framework, we next turned to investigate the anion binding ability of these different cages. Investigations of the anion binding ability of phosphine cage **2** were prevented by the requirement for $Et_3NHCl$ to be present in its synthesis. Extensive anion binding was observed, however, utilizing phosphine oxide cage **3**, phosphonium cage **4**, and guilded cage **5** (Figure 1). Cages **3**, **4** and **5** were found to bind a range of non-coordinating anions, including hexafluorophosphate, tetrafluoroborate, perrhenate, perchlorate, and tosylate in fast exchange on the NMR time scale. Tetraphenylborate was found to bind in fast exchange to **4** and **5**, and in slow exchange to phosphine oxide cage **3** (Figures S14, S15 and S17). Where solubility and stability issues did not prevent their determination, binding constants could be derived from a 1:1 binding model (Supporting Information Section 5). $^1$H NMR signals corresponding to the P-phenyl C-H bonds were seen to move most, whereas those pointing away from the cavity were not observed to move. These observations are consistent with internal binding, rather than counterion exchange. Phosphine oxide cage **3** was observed to bind anions more strongly than either **4** or **5**, with perrhenate being the preferred guest for all three cages.

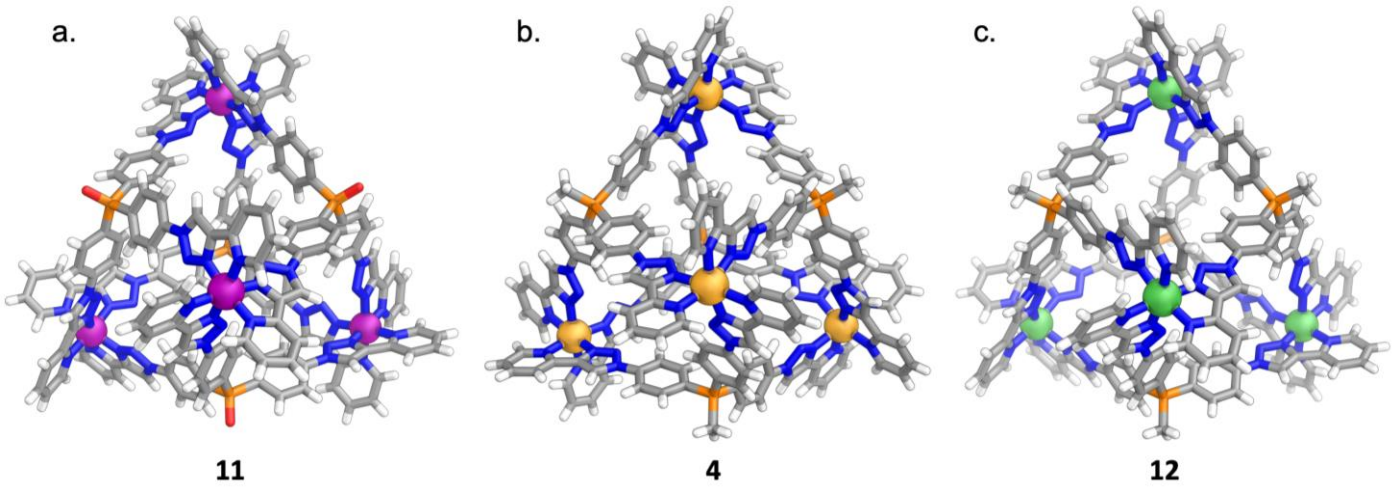


**Figure 3**. Crystal structures of a) $Fe^{II}_4L_4$ phosphine oxide cage **11**; b) $Zn_4L_4$ phosphonium cage **4**; c) $Ni^{II}_4L_4$ phosphonium cage **12**. Counterions, disorder and molecules of solvent of crystallization are omitted for clarity.

Phosphine oxide cage **3** was found to bind to a wider range of guests than phosphonium cage **4** and guilded cage **5**, including chloride, bromide and iodide, as well as trifluoroacetate. The other cages either failed to bind these anions, or decomposed upon treatment with them, in the case of phosphonium cage **4** (Figures S13-S18). This observation was initially surprising, as we had anticipated that phosphonium salt cage **4** would be a better anion binder than phosphonium oxide cage **3**, due to its increased charge of +12, as opposed to +8. We thus infer increased charge repulsion, and inductive withdrawal of electron density away from the triazole-pyridine binding motifs, leads to the destruction of **4** rather than anion binding in the cases of the more coordinating halide and trifluoroacetate anions.

Guilded cage **5** was observed to bind cyanide (Figure S18), whereas the addition of this anion to phosphonium cage **4** and phosphine oxide cage **3** led to the destruction of the cages. We infer that the cyanide displaces chloride at the gold centers, with cyanide known to have high affinity for gold-phosphine complexes.[38] When carbon-13 labelled cyanide was used peaks corresponding to cyanide bound to the gold center were observed, with a $^{13}C$-Au-$^{31}P$ coupling constant of 128.9 Hz, which is consistent with previous reports (Figure S19).[39]

This system of new phosphine-containing cages thus demonstrates how post-assembly modification may tailor binding properties *in situ*. Future work will seek to incorporate such cages into chemical systems, where guest uptake and release is regulated using post-assembly modification.

## ASSOCIATED CONTENT

### Supporting Information

The Supporting Information is available free of charge on the ACS Publications website at DOI: xxxxxxxx. Detailed descriptions of synthetic procedures; characterization of new compounds; spectroscopic data (PDF).

X-ray data for **4** (CCDC 1900372)
X-ray data for **11** (CCDC 1900370)
X-ray data for **12** (CCDC 1900371)

## AUTHOR INFORMATION

### Corresponding Author

*jrn34@cam.ac.uk

### ORCID

Charlie T. McTernan: 0000-0003-1359-0663
Tanya K. Ronson: 0000-0002-6917-3685
Jonathan R. Nitschke: 0000-0002-4060-5122

### Notes

The authors declare no competing financial interest.

## ACKNOWLEDGMENT

This work was supported by the European Research Council (695009) and the UK Engineering and Physical Sciences Research Council (EPSRC, EP/P027067/1). We thank the EPSRC National Mass Spectrometry Centre (Swansea, UK) for high resolution mass spectrometry and Diamond Light Source (UK) for synchrotron beamtime on I19 (MT15768). CTM thanks the Leverhulme and Isaac Newton Trusts, and Sidney Sussex College, Cambridge for Fellowship support.

## REFERENCES

1. Grant, B. J.; Gorfe, A. A.; McCammon, J. A. Large conformational changes in proteins: signaling and other functions. *Curr. Opp. Struct. Biol.* **2010**, *20*, 142–147.
2. Vanyushin, B. F.; Tkacheva, S. G.; Belozersky, A. N. Rare bases in animal DNA. *Nature* **1970**, *225*, 948–949.
3. Vanyushin, B. F.; Belozersky, A. N.; Kokurina, N. A.; Kadirova, D. X. Adenine methylation in eukaryotic DNA. *Nature* **1968**, *218*, 1066–1067.
4. Goldberg, A. D.; Allis, C. D.; Bernstein, E. Epigenetics: a landscape takes shape. *Cell* **2007**, *128*, 635–638.

5. Walsh, C. T.; Garneau-Tsodikova, S.; Gatto, G. J. Protein post-translational modifications: the chemistry of proteome diversifications. *Angew. Chem., Int. Ed.* **2005**, *44*, 7342–7372.
6. Michael, R.; Bron, A. J. The ageing lens and cataract: a model of normal and pathological ageing. *Philos. Trans. R. Soc. Lond. B Biol. Sci.* **2011**, *366*, 1278–1292.
7. Franker, M. A. M.; Hoogenraad, C. C. Microtubule-based transport – basic mechanisms, traffic rules and role in neurological pathogenesis. *J. Cell Sci.* **2013**, *126*, 2319–2329.
8. Groskreutz, D.; Marriott, D.; Gorman, C. *Prehormone Processing Enzymes and Protein Production.* In: *Cell Biology and Biotechnology*. Oka, M. S.; Rupp, R. G. (Eds), Serono Symposia, USA. Springer, New York, NY, **1993**, pp. 76–92.
9. Stoddart, F. J. Mechanically Interlocked Molecules (MIMs) - molecular shuttles, switches, and machines (Nobel Lecture). *Angew. Chem., Int. Ed.* **2017**, *56*, 11094–11125.
10. Erbas-Cakmak, S.; Leigh, D. A.; McTernan, C. T.; Nussbaumer, A. L. Artifical molecular machines. *Chem. Rev.* **2015**, *115*, 10081–10206.
11. a. Boekhoven, J.; Hendriksen, W. E.; Koper, G. J.; Eelkema, R.; van Esch, J. H. Transient assembly of active materials fueled by a chemical reaction. *Science* **2015**, *349*, 1075–1079. b. Zhuang, J.; Gordon, M. R.; Ventura, J.; Li, L.; Thayumanavan, S. Multi-stimuli responsive macromolecules and their assemblies. *Chem. Soc. Rev.* **2013**, *42*, 7421–7435. c. Wang, W.; Wang, Y.-X.; Yang, H.-B. Supramolecular transformations within discrete coordination-driven supramolecular architectures. *Chem. Soc. Rev.* **2016**, *45*, 2656–2693. d. Wang, Q.-Q.; Day, V. W.; Bowman-James, K. Supramolecular encapsulation of tetrahedrally hydrated guests in a tetrahedron host. *Angew. Chem., Int. Ed.* **2012**, *51*, 2119–2123. e. Llinares, J. M.; Powell, D.; Bowman-James, K. Ammonium based anion receptors. *Coord. Chem. Rev.* **2003**, *240*, 57–75.
12. a. Yuan, S.; Chen, Y.-P.; Quin, J.-S.; Lu, W.; Zou, L.; Zhang, Q.; Wang, X.; Sun, X.; Zhou, H.-C. Linker installation: engineering pore environment with precisely placed functionalities in Zirconium MOFs. *J. Am. Chem. Soc.* **2016**, *138*, 8912–8919. b. Shultz, A. M.; Sarjeant, A. A.; Farha, O. K.; Hupp, J. T.; Nguyen, S. T. Post-synthesis modification of a metal–organic framework to form metallosalen-containing MOF materials. *J. Am. Chem. Soc.* **2011**, *133*, 13252–13255.
13. a. Golas, P. L.; Matyjaszewski, K. Marrying click chemistry with polymerization: expanding the scope of polymeric materials. *Chem. Soc. Rev.* **2010**, *39*, 1338–1354. b. Gauthier, M. A.; Gibson, M. I.; Klok, H.-A. Synthesis of functional polymers by post-polymerization modification. *Angew. Chem., Int. Ed.* **2009**, *48*, 48–58.
14. Li, E.; Jie, K.; Zhou, Y.; Zhao, R.; Huang, F. Post-synthetic modification of nonporous adaptive crystals of pillar[4]arene[1]quinone by capturing vaporized amines. *J. Am. Chem. Soc.*, **2018**, *140*, 15070–15079.
15. a. Bandi, S.; Chand, D. K. Cage-to-cage cascade transformations. *Chem. Eur. J.* **2016**, *22*, 10330–10335. b. McConnell, A. J.; Wood, C. S.; Neelakandan, P. P.; Nitschke, J. N. Stimuli-responsive metal-ligand assemblies. *Chem. Rev.* **2015**, *115*, 7729–7793. c. Kim, T. Y.; Vasdev, R. A. S.; Preston, D.; Crowley, J. D. Strategies for reversible guest uptake and release from metallosupramolecular architectures. *Chem. Eur. J.* **2018**, *24*, 14878–14890.
16. a. Cullen, W.; Thomas, K. A.; Hunter, C. A.; Ward, M. D. pH-Controlled selection between one of three guests from a mixture using a coordination cage host. *Chem. Sci.* **2015**, *6*, 4025–4028. b. Cullen, W.; Turega, S.; Hunter, C. A.; Ward, M. D. pH-Dependent binding of guests in the cavity of a polyhedral coordination cage: reversible uptake and release of drug molecules. *Chem. Sci.* **2015**, *6*, 625–631. c. Riddell, I. A.; Smulders, M. M. J.; Clegg, J. K.; Nitschke, J. R. Encapsulation, storage and controlled release of sulfur hexafluoride from a metal–organic capsule. *Chem. Commun.* **2011**, *47*, 457–459.
17. a. Meudtner, R. M.; Hecht, S. Helicity inversion in responsive foldamers induced by achiral halide ion guests. *Angew. Chem., Int. Ed.* **2008**, *47*, 4926–4930. b. Riddell, I. A.; Hristova, Y. R.; Clegg, J. K.; Wood, C. S.; Breiner, B.; Nitschke, J. R. Five discrete multinuclear metal-organic assemblies from one ligand: deciphering the effects of different templates. *J. Am. Chem. Soc.* **2013**, *135*, 2723–2733. c. Busschaert, N.; Caltagirone, C.; Rossom, W. V.; Gale, P. A. Applications of supramolecular anion recognition. *Chem. Rev.* **2015**, *115*, 8038–8155. d. Löffler, S.; Lübben, J.; Krause, L.; Stalke, D.; Dittrich, B.; Clever, G. H. Triggered exchange of anionic for neutral guests inside a cationic coordination cage. *J. Am. Chem. Soc.* **2015**, *137*, 1060–1063. e. Young, M. C.; Holloway, L. R.; Johnson, A. M.; Hooley, R. J. A supramolecular sorting hat: stereocontrol in metal–ligand self-assembly by complementary hydrogen bonding. *Angew. Chem., Int. Ed.* **2014**, *53*, 9832–9836. f. Riddell, I. A.; Smulders, M. M. J.; Clegg, J. K.; Hristova, Y. R.; Breiner, B.; Thoburn, J. D.; Nitschke, J. R. Anion-induced reconstitution of a self-assembling system to express a chloride-binding $Co_{10}L_{15}$ pentagonal prism. *Nat. Chem.* **2012**, *4*, 751–756. g. Brachvogel, R.-C.; Hampel, F.; von Delius, M. Self-assembly of dynamic othoester cryptates. *Nat. Commun.* **2015**, *6*, 7129.
18. Han, M.; Luo, Y.; Damaschke, B.; Gómez, L.; Ribas, X.; Jose, A.; Peretzki, P.; Seibt, M.; Clever, G. H. Light-controlled interconversion between a self-assembled triangle and a rhombicuboctahedral sphere. *Angew. Chem., Int. Ed.* **2016**, *55*, 445–449.
19. Roberts, D. A.; Pilgrim, B. S.; Nitschke, J. R. Covalent post-assembly modification in metallosupramolecular chemistry. *Chem. Soc. Rev.* **2018**, *47*, 626–644.
20. a. Leigh, D. A.; Pritchard, R. G.; Stephens, A. J. A Star of David catenane. *Nat. Chem.* **2014**, *6*, 978–982. b. Wang, M.; Lan, W.-J.; Zheng, Y.-R.; Cook, T. R.; White, H. S.; Stang, P. J. Post-self-assembly covalent chemistry of discrete multicomponent metallosupramolecular hexagonal prisms. *J. Am. Chem. Soc.* **2011**, *133*, 10752–10755. c. Chakrabarty, R.; Stang, P. J. Post-assembly functionalization of organoplatinum(II) metallacycles via copper-free click chemistry. *J. Am. Chem. Soc.* **2012**, *134*, 14738–14741. d. Cook, T. R.; Zheng, Y.-R.; Stang, P. J. Metal-organic frameworks and self-assembled supramolecular coordination complexes: comparing and contrasting the design, synthesis, and functionality of metal-organic materials. *J. Am. Chem. Soc.* **2013**, *113*, 734–777. e. Han, Y.-F.; Jin, G.-X.; Hahn, F. E. Postsynthetic modification of dicarbene-derived metallacycles via photochemical [2 + 2] cycloaddition. *J. Am. Chem. Soc.* **2013**, *135*, 9263–9266. f. Lewis, J. E. M.; Elliott, A. B. S.; McAdam, C. J.; Gordon, K. C.; Crowley, J. D. 'Click' to functionalise: synthesis, characterisation and enhancement of the physical properties of a series of exo- and endo-functionalised $Pd_2L_4$ nanocages. *Chem. Sci.* **2014**, *5*, 1833–1843. g. Lewis, J. E. M.; McAdam, C. J.; Gardiner, M. G.; Crowley, J. D. A facile "click" approach to functionalised metallosupramolecular architectures. *Chem. Commun.* **2013**, *49*, 3398–3400.
21. a. Pilgrim, B. S.; Roberts, D. A.; Lohr, T. G.; Ronson, T. K.; Nitschke, J. R. Signal transduction in a covalent post-assembly modification cascade. *Nat. Chem.* **2017**, *9*, 1276–1281. b. Ronson, T. K.; Pilgrim, B. S.; Nitschke, J. R. Pathway-dependent post-assembly modification of an anthracene-edged $M^{II}_4L_6$ Tetrahedron. *J. Am. Chem. Soc.* **2016**, *138*, 10417–10420.
22. a. Holloway, L. R.; Bogie, P. M.; Lyon, Y.; Julian, R. R.; Hooley, R. J. Stereoselective postassembly CH oxidation of self-assembled metal-ligand cage complexes. *Inorg. Chem.* **2017**, *56*, 11435–11442. b. Roberts, D. A.; Pilgrim, B. S.; Sirvinskaite, G.; Ronson, T. K.; Nitschke, J. R. Covalent post-

assembly modification triggers multiple structural transformations of a tetrazine-edged $Fe_4L_6$ tetrahedron. *J. Am. Chem. Soc.* **2018**, *140*, 9616–9623. c. Brega, V.; Zeller, M.; He, Y.; Lu, H. P.; Klosterman, J. K. Multi-responsive metal–organic lantern cages in solution. *Chem. Commun.* **2015**, *51*, 5077–5080. d. Roberts, D. A.; Castilla, A. M.; Ronson, T. K.; Nitschke, J. R. Post-assembly modification of kinetically metastable $Fe^{II}_2L_3$ triple helicates. *J. Am. Chem. Soc.* **2014**, *136*, 8201–8204. e. Barran, P. E.; Cole, H. L.; Goldup, S. M.; Leigh, D. A.; McGonigal, P. R.; Symes, M. D.; Wu, J.; Zengerle, M. Active-metal template synthesis of a molecular trefoil knot. *Angew. Chem., Int. Ed.* **2011**, *50*, 12280–12284. f. Zhao, D.; Tan, S.; Yuan, D.; Lu, W.; Rezenom, Y. H.; Jiang, H.; Wang, L.-Q.; Zhou, H.-C. Surface functionalization of porous coordination nanocages via click chemistry and their application in drug delivery. *Adv. Mater.* **2011**, *23*, 90–93. g. Carné-Sánchez, A.; Albalad, J.; Grancha, T.; Imaz, I.; Juanhuix, J.; Larpent, P.; Furukawa, S.; Maspoch, D. Postsynthetic covalent and coordination functionalization of rhodium(II)-based metal-organic polyhedra. *J. Am. Chem. Soc.* **2019**, *141*, 4094–4102.

23. Han, M.; Michel, R.; He, B.; Chen, Y.-S.; Stalke, D.; John, M.; Clever, G. H. Light-triggered guest uptake and release by a photochromic coordination cage. *Angew. Chem., Int. Ed.* **2013**, *52*, 1319–1322.
24. Schneider, M. W.; Oppel, I. M.; Griffin, A.; Mastalerz, M. Post-modification of the interior of porous shape-persistent organic cage compounds. *Angew. Chem., Int. Ed.* **2013**, *52*, 3611–3615.
25. Custelcean, R. Anion encapsulation and dynamics in self-assembled coordination cages. *Chem. Soc. Rev.* **2014**, *43*, 1813–1824.
26. a. Jiao, J.; Li, Z.; Qiao, Z.; Li, X.; Liu, Y.; Dong, J.; Jiang, J.; Cui, Y. Design and self-assembly of hexahedral coordination cages for cascade reactions. *Nat. Commun.* **2018**, *9*, 4423. b. Mal, P.; Breiner, B.; Rissanen, K.; Nitschke, J. R. White phosphorus is air-stable within a self-assembled tetrahedral capsule. *Science* **2009**, *324*, 1697–1699. c. Ronson, T. K.; Meng, W.; Nitschke, J. R. Design principles for the optimization of guest binding in aromatic-paneled $Fe^{II}_4L_6$ cages. *J. Am. Chem. Soc.* **2017**, *139*, 9698–9707.
27. a. Pluth, M. D.; Bergman, R. G.; Raymond, K. N. Acid catalysis in basic solution: A supramolecular host promotes orthoformate hydrolysis. *Science* **2007**, *316*, 85–88. b. Cullen, W.; Misuraca, M. C.; Hunter, C. A.; Williams, N. H.; Ward, M. D. Highly efficient catalysis of the Kemp elimination in the cavity of a cubic coordination cage. *Nat. Chem.* **2016**, *8*, 231–236.
28. Zhang, D.; Ronson, T. K.; Mosquera, J.; Martinez, A.; Nitschke, J. R. Selective anion extraction and recovery using a $Fe^{II}_4L_4$ cage. *Angew. Chem., Int. Ed.* **2018**, *130*, 3779–3783.
29. a. Kuijpers, P. F.; Otte, M.; Dürr, M.; Ivanović-Burmazović, I.; Reek, J. N. H.; de Bruin, B. A self-assembled molecular cage for substrate-selective epoxidation reactions in aqueous media. *ACS Catal.* **2016**, *6*, 3106–3112. b. Rizzuto, F. J.; Wood, D. M.; Ronson, T. K.; Nitschke, J. R. Tuning the redox properties of fullerene clusters within a metal-organic capsule. *J. Am. Chem. Soc.* **2017**, *139*, 11008–11011.
30. a. Lui, S.; Shukla, A. D.; Gadde, S.; Wagner, B. D.; Kaifer, A. E.; Isaacs, L. Ternary complexes comprising cucurbit[10]uril, porphyrins, and guests. *Angew. Chem., Int. Ed.* **2008**, *47*, 2657–2660. b. Iglesias, V.; Avei, M. R.; Bruña, S.; Cuadrado, I.; Kaifer, A. E. Binding interactions between a ferrocenylguanidinium guest and cucurbit[n]uril hosts. *J. Org. Chem.* **2017**, *82*, 415–419. c. Rizzuto, F. J.; Pröhm, P.; Plajer, A. J.; Greenfield, J. L.; Nitschke, J. R. Hydrogen-bond-assisted symmetry breaking in a network of chiral metal-organic assemblies. *J. Am. Chem. Soc.* **2019**, *141*, 1707–1715.
31. a. Gramage-Doria, R.; Hessels, J.; Leenders, S. H. A. M.; Tröppner, O.; Dürr, M.; Ivanović-Burmazović, I.; Reek, J. N. H. Gold(I) catalysis at extreme concentrations inside self-assembled nanospheres. *Angew. Chem., Int. Ed.* **2014**, *53*, 13380–13384. b. Riddell, I. A.; Ronson, T. K.; Nitschke, J. R. Mutual stabilisation between $M^{II}_4L_6$ tetrahedra and $M^{II}X_4^{2-}$ metallate guests. *Chem. Sci.* **2015**, *6*, 3533–3537. c. Holloway, L. R.; Bogie, P. M.; Lyon, Y.; Ngai, C.; Miller, T. F.; Julian, R. R.; Hooley, R. J. Tandem reactivity of a self-assembled cage catalyst with endohedral acid groups. *J. Am. Chem. Soc.* **2018**, *140*, 8078–8081. d. Rizzuto, F. J.; Ramsay, W. J.; Nitschke, J. R. Otherwise unstable structures self-assemble in the cavities of cuboctahedral coordination cages. *J. Am. Chem. Soc.* **2018**, *140*, 11502–11509. e. Martí-Centelles, V.; Lawrence, A. L.; Lusby, P. J. High activity and efficient turnover by a simple, self-assembled "Artificial Diels–Alderase". *J. Am. Chem. Soc.* **2018**, *140*, 2862–2868. f. Wang, Q.-Q.; Gonell, S.; Leenders, S. H. A. M.; Dürr, M.; Ivanović-Burmazović, I.; Reek, J. N. H. Self-assembled nanospheres with multiple endohedral binding sites pre-organize catalysts and substrates for highly efficient reactions. *Nat. Chem.* **2016**, *8*, 225–230.
32. a. Burke, M. J.; Nichol, G. S.; Lusby, P. J. Orthogonal selection and fixing of coordination self-assembly pathways for robust metallo-organic ensemble construction. *J. Am. Chem. Soc.* **2016**, *138*, 9308–9315. b. Symmers, P. R.; Burke, M. J.; August, D. P.; Thomson, P. I. T.; Nichol, G. S.; Warren, M. R.; Campbell, C. J.; Lusby, P. J. Non-equilibrium cobalt(III) "click" capsules. *Chem. Sci.* **2015**, *6*, 756–760.
33. a. Okewole, A. I.; Magwa, N. P.; Tshentu, Z. R. The separation of nickel(II) from base metal ions using 1-octyl-2-(2'-pyridyl)imidazole as an extractant in a highly acidic sulfate medium. *Hydrometallurgy* **2012**, *121*, 81–89. b. Venanzi, L. M. Tetrahedral complexes of nickel(II) and the factors determining their formation. *J. Inorg. Nucl. Chem.* **1958**, *8*, 137–142. c. Eaton, D. R.; Zaw, K. Geometry of nickel(II) complexes. *J. Am. Chem. Soc.* **1972**, *94*, 4394–4395.
34. An alternative structure would involve octahedral co-ordination around the nickel(II) center, with two acetonitrile molecules ligating each nickel(II) (these would all have to de-ligate under ESI-MS conditions).
35. Chellmani, A.; Suresh, R. Kinetics and mechanism of oxidation of triphenylphosphine by hydrogen peroxide. *React. Kinet. Catal. L.* **1988**, *37*, 501–505.
36. Seechurn, C. C. C. J.; Kitching, M. O.; Colacot, T. J.; Snieckus, V. Palladium-catalyzed cross-coupling: a historical contextual perspective to the 2010 Nobel Prize. *Angew. Chem., Int. Ed.* **2012**, *51*, 5062–5085.
37. Percástegui, E. G.; Mosquera, J.; Ronson, T. K.; Plajer, A. J.; Kieffer, M.; Nitschke, J. R. Waterproof architectures through subcomponent self-assembly. *Chem. Sci.* **2019**, *10*, 2006–2018.
38. a. Hormann-Arendt, A. L.; Frank Shaw III, C. Ligand-scrambling reactions of cyano(trialkyl/triarylphosphine)gold(I) complexes: examination of factors influencing the equilibrium constant. *Inorg. Chem.* **1990**, *29*, 4683–4687. b. Akhtar. N. M.; Gazi, I. H.; Isab, A. A.; Al-Arfaj, A. R.; Wazeer, M. I. M.; Hussain, M. S. $^{15}N$ and $^{31}P$ NMR studies of cyano(trialkyl/triaryl)phosphine gold (I) complexes. *J. Coord. Chem.* **1995**, *36*, 149–157.
39. We were initially surprised that addition of cyanide did not lead to removal of the gold and formation of $Au(CN)_2^-$. Ref 34 details the synthesis of $R_3PAuCN$ architectures, finding that the process of ligand scrambling leading to $Au(CN)_2^-$ formation is inhibited by low concentrations, the use of aryl phosphines, and more electron deficient phosphines. All three of these effects are operative here, helping to explain why we do not see removal of the gold from the phosphine by cyanide to form $Au(CN)_2^-$ despite its very high stability.

Table of Contents graphic: